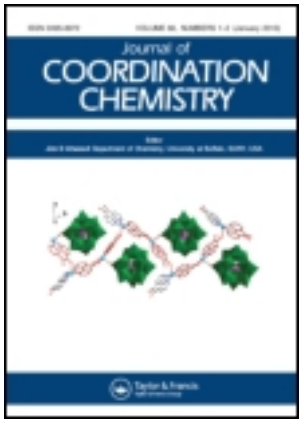

Journal of Coordination Chemistry
Publication details, including instructions for authors and subscription information:
http://www.tandfonline.com/loi/gcoo20

Zinc(II) and copper(II) complexes containing asymmetrical Salamo-type ligands: syntheses, crystal structures, and spectroscopic behaviors

Wen-Kui Dong[a], Yin-Xia Sun[a], Xiu-Yan Dong[a], Si-Jia Xing[a] & Li Wang[a]

[a] School of Chemical and Biological Engineering, Lanzhou Jiaotong University, Lanzhou, P.R. China

Accepted author version posted online: 14 Aug 2013.Published online: 24 Sep 2013.

To cite this article: Wen-Kui Dong, Yin-Xia Sun, Xiu-Yan Dong, Si-Jia Xing & Li Wang (2013) Zinc(II) and copper(II) complexes containing asymmetrical Salamo-type ligands: syntheses, crystal structures, and spectroscopic behaviors, Journal of Coordination Chemistry, 66:18, 3291-3304, DOI: 10.1080/00958972.2013.834426

To link to this article: http://dx.doi.org/10.1080/00958972.2013.834426

Journal of Coordination Chemistry, 2013
Vol. 66, No. 18, 3291–3304, http://dx.doi.org/10.1080/00958972.2013.834426

Zinc(II) and copper(II) complexes containing asymmetrical Salamo-type ligands: syntheses, crystal structures, and spectroscopic behaviors

WEN-KUI DONG*, YIN-XIA SUN, XIU-YAN DONG, SI-JIA XING and LI WANG

School of Chemical and Biological Engineering, Lanzhou Jiaotong University, Lanzhou, P.R. China

(*Received 3 June 2013; accepted 31 July 2013*)

$[Zn_4(L^1)_2(OAc)_2(CH_3CH_2OH)_2]$ and $[CuL^2(H_2O)]$ with new asymmetric Salamo-type ligands have been synthesized and characterized. There are two coordination geometries (trigonal bipyramidal and square pyramidal) in the Zn(II) complex, and the Cu(II) complex has square-pyramidal geometry. A self-assembling continual zigzag chain is formed by intermolecular hydrogen bonds in the Cu(II) complex. The self-assembling array of the Zn(II) complex is linked by intermolecular C–H···O and C–H···π interactions. Blue emissions of the Zn(II) and Cu(II) complexes in DMF solution are exhibited by fluorescence.

Keywords: Asymmetric Salamo-type ligand; Transition metal complex; Synthesis; Crystal structure; Spectroscopic behavior

1. Introduction

Transition metal complexes with Salen-type ligands have attracted much interest for their catalytic activities [1, 2], especially in asymmetric catalysis [3, 4], biological activity, such as anticancer [5] and fluorescence characteristics [6, 7]. Photoluminescence of coordination complexes has applications in luminescent devices [8, 9], observed for Salen-type compounds and their transition metal complexes [10–14]. Zn(II) and Cu(II) complexes with Salen-type ligands draw attention for their photoluminescence [15–17]. Excellent work has synthesized mononuclear, homo-, or heterodinuclear transition metal complexes bearing symmetric Salen-type bisoxime ligand or its derivatives [18].

The current work stems from our interest in asymmetric Salamo-type bisoximes. Compared with symmetric Salamo-type bisoxime ligands, composition (R^1-CH=N–O–$(CH)_n$–O–N=CH-R^2) is unusual. Selective synthesis of asymmetrical Salamo-type ligands is important because electronic and steric effects of the ligands on Salen-metal-assisted catalysis may be controlled by introduction of different substituents into the benzene rings [19]. Asymmetric configuration with Salamo-type ligands would afford greater structural variation and coordination polymers [20, 21] and would be expected to lead to novel

*Corresponding author. Email: dongwk@126.com

characteristics. Metal complexes derived from asymmetrical Salamo-type ligands sometimes exhibit better enantioselectivities when compared with their symmetric counterparts [22].

To study the structures and fluorescent characteristics of complexes with asymmetric Salamo-type ligands, herein, we report the synthesis, characterization, and crystal structures of $[Zn_4(L^1)_2(OAc)_2(CH_3CH_2OH)_2]$ with H_3L^1 (4-chloro-6′-hydroxy-2,2′[ethylenediyldioxy-bis(nitrilomethylidyne)]diphenol) and $[CuL^2(H_2O)]$ with H_2L^2 (4-chloro-6′methoxy-2,2′-[ethylenediyldioxybis(nitrilomethylidyne)]diphenol).

2. Experimental

2.1. *Materials and methods*

2-Hydroxy-5-chlorobenzaldehyde, 2-hydroxy-3-methoxybenzaldehyde, and 2,3-dihydroxybenzaldehyde were purchased from Aldrich and used without purification; other reagents and solvents were analytical grade reagents from Tianjin Chemical Reagent Factory.

Elemental analyses for Cu and Zn were carried out by an IRIS ER/S·WP-1 ICP atomic emission spectrometer and C, H, and N analyses with a GmbH Variuo EL V3.00 automatic elemental analyzer. IR spectra were recorded on a Vertex70 FT-IR spectrophotometer, with samples prepared as KBr (500–4000 cm^{-1}) and CsI (100–500 cm^{-1}) pellets. UV–vis absorption and fluorescence spectra were recorded on a Shimadzu UV-2550 spectrometer and Perkin–Elmer LS-55 spectrometer, respectively. TG-DTA analyses were carried out at a heating rate of 5 °C min^{-1} on a ZRY-1P thermoanalyzer. ^1H NMR spectra were recorded on a Mercury-400B spectrometer. X-ray single-crystal structures were determined on a Bruker Smart 1000 CCD area detector. Melting points were measured with a microscopic melting point apparatus made in Beijing Taike Instrument Limited Company, and the thermometer was uncorrected.

2.2. *Synthesis and X-ray crystallography*

The synthetic route of two ligands is shown in scheme 1.

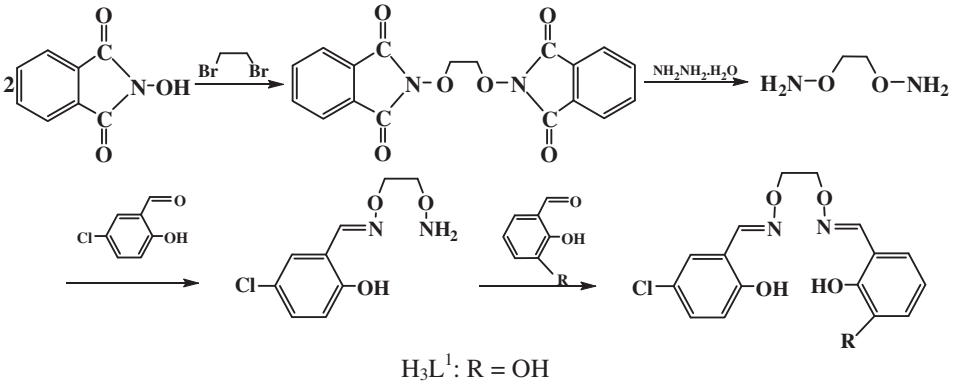

H_3L^1: R = OH

H_2L^2: R = OCH_3

Scheme 1. The synthetic route of two asymmetric Salen-type ligands.

2.2.1. Synthesis and characterization of H_3L^1. 1,2-Bis(aminooxy)ethane was synthesized by a similar method [17, 20]. Yield: 77.2%. Anal. Calcd for $C_2H_8N_2O_2$ (%): C, 26.08; H, 8.76; N, 30.42. Found (%): C, 25.92; H, 8.87; N, 30.35.

2.2.1.1. 2-[O-(1-ethyloxyamide)]oxime-4-chlorophenol. A solution of 5-chloro-2hydroxybenzaldehyde (3 mM) in ethanol (20 mL) was added to a solution of 1,2bis(aminooxy)ethane (6 mM) in ethanol (10 mL), and the mixture was heated at 50–55 °C for 5 h. The solution was concentrated in vacuo, and the residue was purified by column chromatography (SiO_2, chloroform/ethyl acetate, 50 : 2) to afford crystals of the monoxime compound. Yield: 67.3%. Anal. Calcd for $C_9H_{11}ClN_2O_3$ (%): C, 46.87; H, 4.81; N, 12.15. Found (%): C, 46.71; H, 4.95; N, 12.01. m.p. 67–68 °C. ^{1}H NMR (400 MHz, $CDCl_3$) δ: 3.97 (t, J = 4.5 Hz, 2H), 4.38 (t, J = 4.5 Hz, 2H), 5.54 (brs, 2H), 6.88 (d, J = 9.0 Hz, 1H), 7.26 (d, J = 2.5 Hz, 1H), 7.36 (dd, J = 9.0, 2.5 Hz, 1H), 8.12 (s, 1H), 9.86 (s, 1H).

2.2.1.2. 4-Chloro-6′-hydroxy-2,2′-[ethylenediyldioxybis(nitrilomethylidyne)]diphenol (H_3L^1). A solution of 2-[*O*-(1-ethyloxyamide)]oxime-4-chlorophenol (1 mM) in ethanol (10 mL) was added to a solution of 2,3-dihydroxybenzaldehyde (1 mM) in ethanol (10 mL), and the mixture was heated at 50–55 °C for 5 h. After cooling to room temperature, white precipitate was collected on a suction filter to give colorless powder, unlike yellowish H_2Salen analogues. Yield: 78.8%. m.p. 104–105 °C. Anal. Calcd for $C_{16}H_{15}ClN_2O_5$ (%): C, 54.79; H, 4.31; N, 7.99. Found: C, 54.96; H, 4.22; N, 7.96. ^{1}H NMR (400 MHz, DMSO-d6, d, ppm) δ: 4.48–4.50 (m, 4H, CH_2), 6.88 (d, J = 8.6 Hz, 1H), 6.92 (t, J = 7.8 Hz, 1H), 6.98 (d, J = 7.8 Hz, 1H), 7.16 (dd, J = 7.8 Hz, 1.5 Hz, 1H), 7.26 (d, J = 2.5 Hz, 1H), 7.35 (dd, J = 8.6 Hz, 2.5 Hz, 1H), 8.16 (s, 1H), 8.23 (s, 1H), 9.72 (s, 1H), 9.77 (s, 1H), 10.38 (s, 1H).

2.2.2. Synthesis and characterization of H_2L^2. 4-Chloro-6′-methoxy-2,2′[ethylenediyldioxybis(nitrilomethylidyne)]diphenol (H_2L^2) was synthesized by a similar method. Yield: 73.6%. m.p. 106–107 °C. Anal. Calcd for $C_{17}H_{17}ClN_2O_5$ (%): C, 55.97; H, 4.70; N, 7.68. Found: C, 56.21; H, 4.59; N, 7.66. ^{1}H NMR (400 MHz, DMSO-d6, d, ppm) δ: 3.91 (s, 3H), 4.47–4.49 (m, 4H, CH_2), 6.89 (d, J = 8.6 Hz, 1H), 6.91 (t, J = 7.8 Hz, 1H), 6.97 (d, J = 7.8 Hz, 1H), 7.15 (dd, J = 7.8 Hz, 1.5 Hz, 1H), 7.27 (d, J = 2.5 Hz, 1H), 7.34 (dd, J = 8.6 Hz, 2.5 Hz, 1H), 8.15 (s, 1H), 8.21 (s, 1H), 9.70 (s, 1H), 9.74 (s, 1H), 10.38 (s, 1H).

2.2.3. Synthesis of $[Zn_4(L^1)_2(OAc)_2(CH_3CH_2OH)_2]$. The procedure described [21] was used except using H_3L^1 (17.6 mg) and ethanol (12 mL) and THF/ethanol (1 : 4, 15 mL). Yield: 20.12%. Anal. Calcd for $C_{40}H_{42}Cl_2N_4O_{16}Zn_4$ (%): C, 41.16; H, 3.63; N, 4.80; Zn, 22.41. Found: C, 41.01; H, 2.68; N, 4.95; Zn, 22.19.

2.2.4. Synthesis and characterization of $[CuL^2(H_2O)]$. Detailed synthesis for $[CuL^2(H_2O)]$: A solution of Cu(II) acetate hydrate (20.0 mg, 0.1 mM) in ethanol (10 mL) was added dropwise to a solution of H_2L^2 (36.5 mg, 0.1 mM) in acetone/ethanol (1 : 2) (15 mL) at room temperature. The color of the solution turned brown immediately, the mixture was filtered and the filtrate was allowed to stand at room temperature for two weeks. The solvent was partially evaporated, and brown needle-like single crystals suitable

Table 1. Crystal data and structure refinement for the Zn(II) and Cu(II) complexes.

CCDC deposit number	864126	864127
Empirical formula	$C_{40}H_{42}Cl_2N_4O_{16}Zn_4$	$C_{17}H_{17}ClCuN_2O_6$
Formula weight	1167.16	444.32
Temperature (K)	298(2)	293(2)
Wavelength (Å)	0.71073	0.71073
Crystal system	Triclinic	Orthorhombic
Space group	*P-1*	*Iba2*
Unit cell dimensions		
a (Å)	8.9686(9)	19.400(2)
b (Å)	11.4814(11)	25.099(3)
c (Å)	12.3957(12)	7.4424(5)
α (°)	92.8420(10)	90
β (°)	107.945(2)	90
γ (°)	105.501(2)	90
V (Å^3)	1158.0(2)	3623.9(6)
Z	1	8
D_{Calc} (Mg m^{-3})	1.674	1.629
μ (mm^{-1})	2.235	1.390
F (000)	592	1816
Crystal size (mm)	0.31 × 0.13 × 0.08	0.40 × 0.17 × 0.08
θ range (°)	2.64–25.02	2.65–25.02
Index ranges	$-10 \le h \le 10$, $-12 \le k \le 13$, $-14 \le l \le 14$	$-23 \le h \le 18$, $-29 \le k \le 23$, $-5 \le l \le 8$
Reflections collected	5988	4969
Independent reflections	4041	2343
R_{int}	0.0693	0.0461
Completeness to $\theta = 25.02$ (%)	98.8	99.8
Data/restraints/parameters	4041/0/320	2343/1/245
Goodness of fit (GOF)	1.021	1.022
R_1	0.0743	0.0390
wR_2 [$I > 2\sigma(I)$]	0.1722	0.0703
$\Delta\rho_{max,\ min}$ (e Å^{-3})	0.907 and −0.610	0.410 and −0.255

for X-ray crystallographic analysis were obtained. Yield: 17.45%. Anal. Calcd for $C_{17}H_{17}ClCuN_2O_6$ (%): C, 45.95; H, 3.86; N, 6.30; Cu, 14.30. Found: C, 46.26; H, 3.69; N, 6.35; Cu, 14.09.

2.2.5. X-ray crystallography of the Zn(II) and Cu(II) complexes. The single crystals of the Zn(II) and Cu(II) complexes with approximate dimensions 0.31 × 0.13 × 0.08 and 0.40 × 0.17 × 0.08 mm were placed on a Bruker Smart 1000 CCD area detector. The diffraction data were collected using graphite-monochromated MoK_α radiation (λ = 0.71073 Å) at 298(2) K and 293(2) K. The structures were solved using SHELXL-97 and Fourier difference techniques and refined by full-matrix least-squares on F^2. All hydrogens were added theoretically. The crystal and experimental data are shown in table 1.

3. Results and discussion

3.1. *X-ray crystal structures*

The crystal structures of the Zn(II) and Cu(II) complexes are shown in figures 1 and 2, respectively. The crystal data and experimental details are given in table 1; selected bond lengths and angles of the two complexes are listed in table 2.

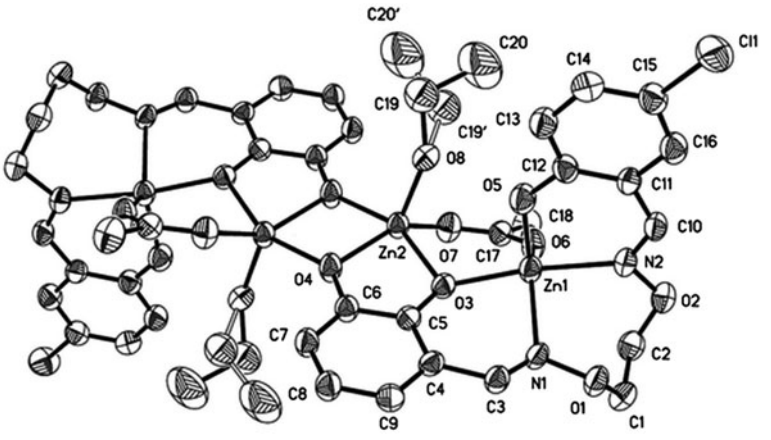

Figure 1. Molecular structure of Zn(II) complex with atom numbering. Thermal ellipsoids are plotted at 30% probability level.

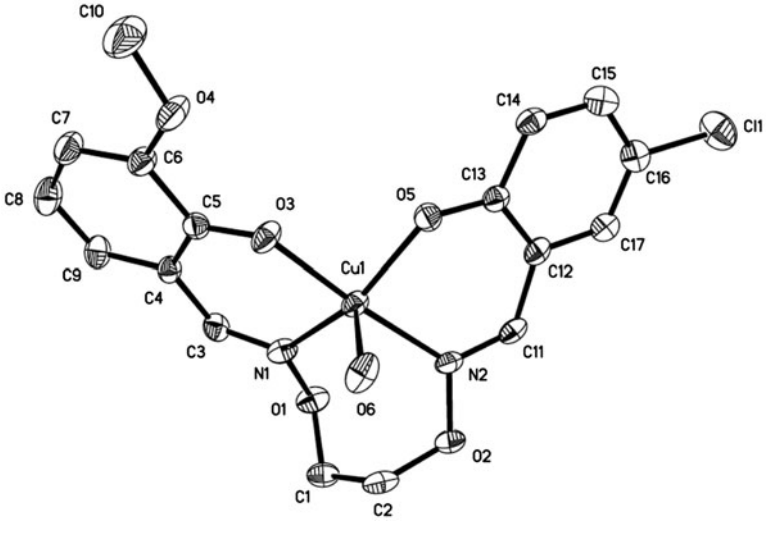

Figure 2. Molecular structure of Cu(II) complex with atom numbering. Thermal ellipsoids are plotted at 30% probability level.

If hydroxyl groups are introduced to the 3 position of salicylidene moieties of Salen-type ligands, highly versatile coordination ability is expected. This versatility is due to the two neighboring hydroxyl groups at the 2 and 3 positions, which can act as a catecholato^{2-} ligand when they are deprotonated. Indeed, 3-hydroxysalen derivatives form a variety of metal complexes such as mononuclear [23–36], dinuclear [37], trinuclear [38], and hetero-metallic 3d-4f or 3d-5f complexes [27–36]. Coordination of 3-hydroxysalen-type ligands to metals in a divergent fashion leads to serendipitous formation of Zn_8 clusters [16]. In most cases, however, the structure and properties in solution were not thoroughly investigated because of low solubility or instability.

Table 2. Selected bond distances (Å) and angles (°) for the Zn(II) and Cu(II) complexes.

Bond	Distance	Bond	Distance	Bond	Distance
Zn(II) complex					
Zn1–O5	1.946(6)	Zn1–N2	2.110(7)	Zn2–O4	2.022(6)
Zn1–O6	1.968(6)	Zn2–O7	1.974(6)	Zn2–O3	2.038(5)
Zn1–O3	1.987(6)	Zn2–O4$^{\#1}$	1.976(5)	Zn2–Zn2$^{\#1}$	3.114(2)
Zn1–N1	2.090(7)	Zn2–O8	2.018(6)		
Cu(II) complex					
Cu1–O3	1.918(4)	Cu1–N1	1.991(5)	Cu1–O6	2.238(4)
Cu1–O5	1.934(4)	Cu1–N2	2.006(4)		
Bond	Angle	Bond	Angle	Bond	Angle
Zn(II) complex					
O5–Zn1–O6	111.2(3)	N1–Zn1–N2	87.9(3)	O4$^{\#1}$–Zn2–O3	155.6(2)
O5–Zn1–O3	95.1(2)	O7–Zn2–O4$^{\#1}$	97.5(2)	O8–Zn2–O3	92.1(2)
O6–Zn1–O3	93.1(2)	O7–Zn2–O8	106.2(3)	O4–Zn2–O3	79.4(2)
O5–Zn1–N1	118.3(3)	O4$^{\#1}$–Zn2–O8	103.5(3)	O7–Zn2–Zn2$^{\#1}$	127.4(2)
O6–Zn1–N1	130.5(3)	O7–Zn2–O4	143.9(3)	O4$^{\#1}$–Zn2–Zn2$^{\#1}$	39.4(2)
O3–Zn1–N1	84.8(2)	O4$^{\#1}$–Zn2–O4	77.7(3)	O8–Zn2–Zn2$^{\#1}$	111.5(2)
O5–Zn1–N2	88.6(3)	O8–Zn2–O4	109.7(3)	O4–Zn2–Zn2$^{\#1}$	38.3(2)
O6–Zn1–N2	91.5(3)	O7–Zn2–O3	96.0(2)	O3–Zn2–Zn2$^{\#1}$	117.3(2)
O3–Zn1–N2	172.6(3)				
Cu(II) complex					
O3–Cu1–O5	87.1(2)	O5–Cu1–N2	88.7(2)	O5–Cu1–O6	93.4(2)
O3–Cu1–N1	88.9(2)	N1–Cu1–N2	94.4(2)	N1–Cu1–O6	113.8(2)
O5–Cu1–N1	152.5(2)	O3–Cu1–O6	90.4(2)	N2–Cu1–O6	90.8(2)
O3–Cu1–N2	175.7(2)				

Symmetry transformations used to generate equivalent atoms for the Zn(II) complex, $^{\#1}$ $-x+1, -y+1, -z+1$.

The Zn(II) complex crystallizes in the triclinic system, space group *P-1*. Assembly of four Zn(II) ions, two $(L^1)^{3-}$, two acetates, and two coordinated ethanols result in a tetranuclear Zn(II) complex. This tetranuclear metal complex is unusual for Salen- or Salamo-type complexes [21], demonstrating that the complexation of 3-hydroxy Salamo-type ligands with Zn(II) acetate takes place cooperatively [16, 21], unlike in the case of other substituted Salen- [23–38] or Salamo-type ligands [17]. In fact, the structure of this tetranuclear Zn(II) complex is very similar with the Zn(II) complex previously reported [21]. The structure can be described as two $[Zn_2L^1(OAc)(CH_3CH_2OH)]$ units connected with two diphenoxy-bridges. In each unit, the Zn1 center was coordinated through N_2O_2 donors. The central Zn2 was coordinated by three deprotonated μ-phenolic oxygens in two $[ZnL^1]$ chelates and one oxygen of coordinated ethanol. Acetate coordinates to two Zn(II) ions via Zn1–O–C–O–Zn2 bridge. Thus, the complex contains four five-coordinate Zn(II) centers. Zn1 is a trigonal bipyramidal geometry with O3 and N2 axial ($\tau = 0.702$), and Zn2 is square pyramidal ($\tau = 0.195$) [39] with O8 axial from coordinated ethanol, similar with the coordination geometries of Zn(II) in the literature [21]. The difference is the bond lengths and angles between the central atom and the coordination groups, as well as the distortions of the geometries of the Zn(II) centers.

Zn1 is nearly coplanar with the plane (O6–N1–O5) deviating from the mean plane by 0.024(3) Å. The Zn1–N2 bond length to the apical nitrogen is 2.110(7) Å, about 0.020 Å longer than the bond length between Zn(II) and the basal nitrogen Zn1–N1 (2.090(7) Å). The axial bond length Zn1–O3 (1.987(6) Å) is also longer by 0.019(3) Å than the Zn1–O6 bond length (1.968(6) Å) and by 0.041(3) Å than the Zn1–O5 bond length (1.946(6) Å).

The dihedral angle between the coordination planes of N1–Zn1–O3 and N2–Zn1–O5 is 61.64(3), larger than that of reported complexes with symmetric Salen-type bisoxime ligands [40]. This significant enlargement indicates $(L^1)^{3-}$ has serious distortion, probably as a result of the asymmetry. The geometry of Zn2 is different from Zn1 as a square pyramid. The four donors (O3, O4, $O4^{\#1}$, and O7) in the basal plane deviate slightly from the mean plane (O3 and $O4^{\#1}$ above by 0.174(3) Å and 0.181(3) Å, O4 and O7 below by 0.207(3) Å and 0.148(3) Å, respectively); Zn2 lies 0.442(3) Å above the plane. The Zn2–O8 bond distance to the apical O8 is 2.018(6) Å. Basal Zn2–O3 and Zn2–O4 bond lengths (2.038(5) Å and 2.022(6) Å) are longer than Zn2–O7 and Zn2–$O4^{\#1}$ (1.974(6) Å and 1.976 (5) Å). The dihedral angle between the planes of O7–Zn2–O3 and O4–Zn2–$O4^{\#1}$ is 38.56 (3)°. Zn2 and $Zn2^{\#1}$ are connected with two μ-phenolic oxygens (O4 and $O4^{\#1}$). Zn2, O4, $Zn2^{\#1}$, and $O4^{\#1}$ constitute a parallelogram. Two kinds of coordination geometry (trigonal bipyramidal and square pyramidal) are contained in the Zn(II) complex.

The Zn(II) complexes are linked by intermolecular hydrogen bonds. Hydrogen bond data are summarized in table 3. There is a strong intramolecular O8–H8C···O5 hydrogen bond in the Zn(II) complex. Zn(II) monomers are linked by four intermolecular C18–H18C···O3, four C1–H1A···$\pi_{centroid(C4–C9)}$, and four C18–H18C···$\pi_{centroid(C4–C9)}$ hydrogen bond interactions into an infinite 1-D supramolecular chain along the *a*-axis (figure 3(a)). This linkage is further stabilized by two pairs of intermolecular C1–H1B···O1 hydrogen bonds and two pairs of C18–H18A···$\pi_{centroid(C11–C16)}$ interactions to form an infinite 2-D-layer (figure 3(b)). Thus, every Zn(II) complex links eight other adjacent molecules into a 3-D supramolecular network structure through intermolecular C–H···O and C–H···π interactions (figure 3(c)), entirely different from the 1-D-chain supramolecular structure reported [21]. Changes of the substituents on the ligand have little effect on the structure of Zn(II) complexes, but a greater impact on the supramolecular structure of the Zn(II) complexes.

The X-ray crystal structure shows that the molecular structure of the Cu(II) complex consists of one Cu(II), one $(L^2)^{2-}$, and one coordinated water. The value of $\tau = 0.386$ clearly indicates that Cu(II) is close to square-pyramidal topology with donors N_2O_2 (Cu1–O3: 1.918(4) Å; Cu1–O5: 1.934(4) Å; Cu1–N1: 1.991(5) Å; Cu1–N2: 2.006(4) Å) forming a basal plane and the axial site occupied by O(6) from water (Cu1···O6, 2.238(4) Å). The axial Cu1···O6

Table 3. Hydrogen bonding distances (Å) and angles (°) for the Zn(II) and Cu(II) complexes.

D–H···A	d(D–H)	d(H···A)	d(D..A)	∠D–H···A
Zn(II) complex				
O8–H8C···O5	0.820	1.823	2.635(3)	171
C1–H1A···$\pi_{centroid(C4–C9)}$	0.970	3.555	4.009(3)	111
C1–H1B···O1	0.970	2.686	3.308(3)	122
C18–H18A···$\pi_{centroid(C11–C16)}$	0.960	3.318	3.985(4)	128
C18–H18C···O3	0.959	2.671	3.442(3)	138
C18–H18C···$\pi_{centroid(C4–C9)}$	0.959	3.288	3.946(3)	127
Cu(II) complex				
O6–H6C···O3	0.849	2.549	2.941(3)	109
O6–H6C···O4	0.850	2.094	2.943(3)	177
O6–H6D···O3	0.850	2.589	2.941(3)	106
O6–H6D···O5	0.850	1.941	2.789(3)	176
C1–H1A···O1	0.970	2.628	3.465(3)	145
C2–H2B···O5	0.970	2.601	3.520(3)	158
C10–H10B···O4	0.960	2.625	3.470(3)	147
C8–H8···Cl1	0.929	2.911	3.585(3)	130
C17–H17···Cl1	0.931	2.859	3.594(3)	137

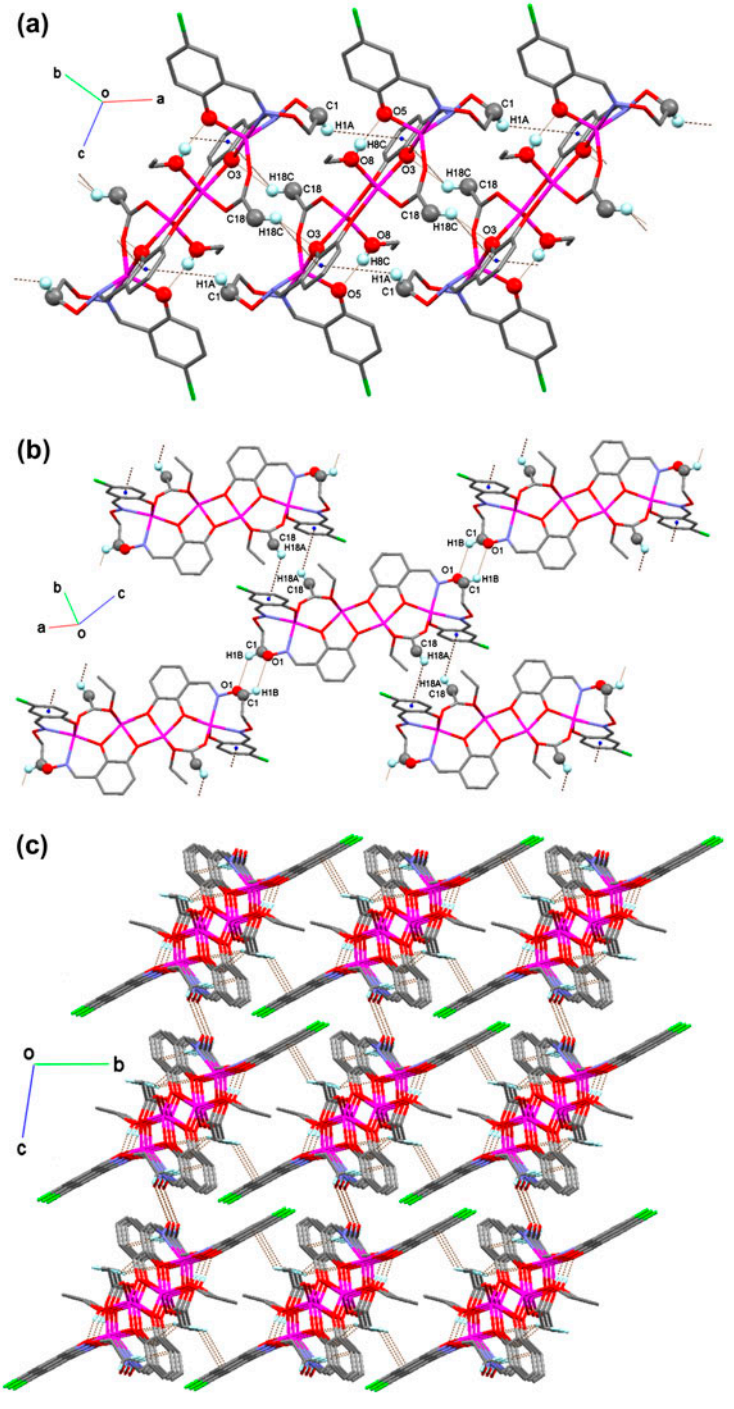

Figure 3. Supermolecular structure of $[Zn_4L^1{}_2(OAc)_2(CH_3CH_2OH)_2]$. (a) View of the 1-D chain motif within the Zn(II) complex along the *a*-axis; (b) view of the 2-D layered motif along the *ac* plane for the Zn(II) complex; (c) part of 3-D supramolecular network through intermolecular C–H···O and C–H···π interactions for the Zn(II) complex.

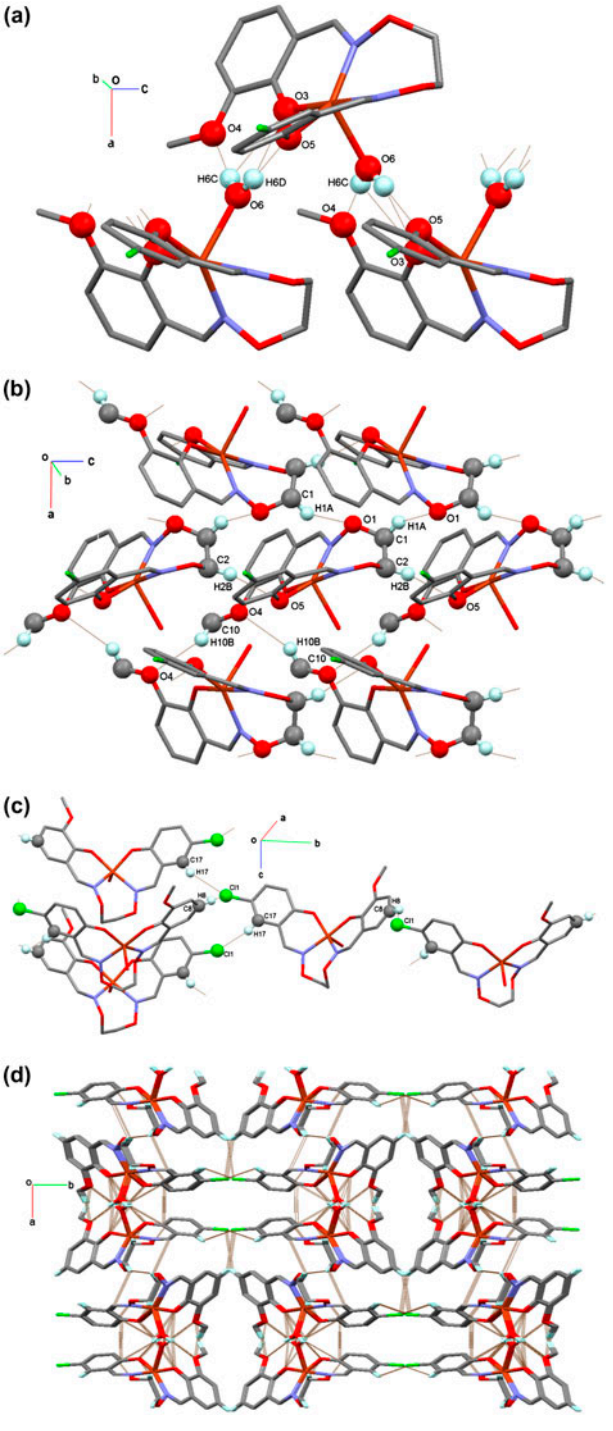

Figure 4. Supermolecular structure of $[CuL^2(H_2O)]$. (a) View of the 1-D chain motif within the Cu(II) complex along the *c*-axis; (b) view of the 2-D layered motif along the *ac* plane for the Cu(II) complex; (c) view of the 1-D chain motif within the Cu(II) complex along the *b* axis; (d) part of 3-D supramolecular network via intermolecular hydrogen bond interactions for the Cu(II) complex.

bond distance is longer than those of the basal plane. Typical Cu–O bond length to apical water in a square-pyramidal molecule is 2.262(6) found in [Cu(MeO–Salen)(H_2O)] [41].

Coordination atoms in the basal plane deviate slightly from the mean plane, with O3 and N2 above average by 0.226(3) Å and 0.202(3) Å, O5 and N1 below average by 0.225(3) Å and 0.203(3) Å. The Cu(II) is displaced 0.248(3) Å from the mean plane. The dihedral angle between the O3–Cu1–N1 and O5–Cu1–N2 coordination planes is 27.27(3), attributed to the asymmetric composition.

The coordinated water in the Cu(II) complex assembles monomeric units by intermolecular hydrogen bonds. As illustrated in figure 4(a), four intermolecular hydrogen bonds, O6–H6D···O3, O6–H6D···O5, O6–H6C···O3, and O6–H6C···O4, are formed. One water proton –O6H6D of the coordinated water in the Cu(II) complex is bound to both coordinated phenolic oxygens (O3 and O5) of $(L^2)^{2-}$ of the adjacent molecules. The other of water proton –O6H6C of coordinated water is bound to coordinated phenolic oxygen O3 and O4 in methoxy of $(L^2)^{2-}$ of the adjacent molecule. Consequently, a zigzag chain along the *c*-axis is formed by intermolecular hydrogen bonds with the nearest Cu···Cu distance of 5.873(3) Å. The molecules further link six other adjacent molecules into an infinite 2-D–layer in the *ac* crystallographic plane by three pairs of intermolecular C1–H1A···O1, C2–H2B···O5, and C10–H10B···O4 hydrogen bonds (figure 4(b)). This linkage is further stabilized by two pairs of intermolecular C8–H8···Cl1 and C17–H17···Cl1 hydrogen bonds (figure 4(c)). Thus, every Cu(II) complex links 10 other molecules into an infinite 3-D supramolecular network via intermolecular O–H···O, C–H···O, and C–H···Cl hydrogen bond interactions (figure 4(d)).

3.2. *Thermal properties*

Thermal decomposition of the Zn(II) complex can be divided into three stages. The initial weight loss occurs from 202.3 to 215.6 °C as an endothermic peak, with 7.5% weight loss (7.9%, calculated) for loss of two coordinated ethanols. The Zn(II) complex does not melt but decomposes at 208.6 °C, higher than the ligand H_3L^1 (*ca*. 187.7 °C). The second stage degradation is 284.7–341.3 °C with mass loss of 10.4% in the TG curve and two violently exothermic peaks in the DTA curve for two coordinated acetates decomposed (theoretical loss of 10.1%). The third strong exothermic peak at 436.2 °C leads to ZnO with a residual value of 22.8% (theoretical 22.4%) when the temperature is above 800 °C.

The thermal analysis curve of the Cu(II) complex indicates only two weight loss stages. The first weight loss from 197.0 to 246.5 °C as 3.9% is in agreement with the calculated 4.1% for loss of one coordinated water. The loss of ligand unit occurs at 380.2 and 423.8 °C in the TG curve and two exothermic peaks in the DTA curve. The final solid product at 561.8 °C may be CuO with a residual value of 14.5%, which matches well with theoretical residual value (14.3%).

3.3. *Spectroscopic behaviors*

3.3.1. IR spectra. IR spectra of H_3L^1, H_2L^2 and their corresponding complexes exhibit various bands from 500 to 4000 cm^{-1}. The free ligands exhibit C=N stretch at 1615 and 1616 cm^{-1}, while $\nu_{C=N}$ of their Zn(II) and Cu(II) complexes is observed at 1606 and 1608 cm^{-1}. The C=N stretch is shifted to a lower frequency by *ca.* 9 and 8 cm^{-1} upon complexation, indicating a decrease in coordination bonds of oxime nitrogen [42].

The Ar–O is a strong band at 1263–1213 cm^{-1} as reported for similar ligands [43–45]. This band occurs at 1261 and 1230 cm^{-1} for H_3L^1 and H_2L^2, respectively, and at 1212 and 1198 cm^{-1} for the Zn(II) and Cu(II) complexes. The shift to lower frequency indicates that M–O bonds formed between metal and phenol [42]. Infrared spectrum of the Zn(II) complex shows the expected strong absorption due to ν(O–H) at *ca*. 3431 cm^{-1}, evidence for the existence of ethanol. The expected strong absorptions in the Cu(II) complex were observed at 3422, 1630, and *ca*. 550 cm^{-1}, respectively, indicating the presence of coordinated water [46].

Far-infrared spectra of the Zn(II) and Cu(II) complexes from 500 to 100 cm^{-1} identify frequencies due to M–O and M–N. The Zn(II) complex showed $\nu_{(Zn-N)}$ and $\nu_{(Zn-O)}$ at 472 and 421 cm^{-1} [46], respectively, and the Cu(II) complex showed $\nu_{(Cu-N)}$ and $\nu_{(Cu-O)}$ at 475 and 437 cm^{-1}, respectively [47]. As pointed out by Percy and Thornton [48], the metal-oxygen and metal-nitrogen frequency assignments are at times very difficult.

3.3.2. UV–vis absorption spectra. The UV–vis absorption spectra of H_3L^1, H_2L^2 and their corresponding complexes in 5.0×10^{-5} mol L^{-1} DMF solution are shown in Supplementary material. The electronic absorption spectrum of Salen-type bisoxime ligand H_3L^1 consists of two relatively intense bands at 270 and 323 nm (271 and 322 nm for H_2L^2), assigned to π–π* transitions of the benzene ring of salicylaldehyde and the oxime, respectively [49]. Upon coordination of the ligands, the absorption at 323 nm disappears from UV–vis spectra of the Zn(II) and Cu(II) complexes, indicating that the oxime nitrogen is involved in coordination [50]. The intraligand π–π* transition of the benzene ring of salicylaldehyde is slightly shifted in the corresponding complexes and appears at 284 and 299 nm for the Zn(II) complex (281 nm for the Cu(II) complex). New bands at 365 and 377 nm for the Zn(II) and Cu(II) complexes are assigned to L→M charge-transfer transition, characteristic of transition metal complexes with N_2O_2 coordination [51].

3.3.3. Fluorescence properties. Fluorescent properties of H_3L^1 and its corresponding Zn(II) complex were investigated at room temperature (figure 5(a)). The ligand exhibits an intense emission at 390 nm upon excitation at 330 nm, which should be assigned to intraligand π–π* transition [52]. The Zn(II) complex shows an intense broad photoluminescence with maximum emission at *ca*. 410 nm upon excitation at 335 nm, slightly red shifted to that of H_3L^1. Since the emission peak position of the Zn(II) complex is similar to that of free ligand, the emission peak in the spectrum of the Zn(II) complex may also arise from the intraligand transition. No emission originating from metal-centered or metal-to-ligand/ligand-to-metal charge-transfer excited states are expected for the d^{10} Zn(II). Thus, the emission observed in the Zn(II) complex is tentatively assigned to the (π–π*) intraligand fluorescence.

Emission spectra of H_2L^2 and its Cu(II) complex are shown in figure 5(b). In comparison with H_2L^2 with maximum emission wavelength at 380 nm when excited at 330 nm, the Cu(II) complex exhibits red shift with the maximum emission wavelength λ_{max} = 429 nm when excited at 345 nm, assigned to ligand-to-metal charge transfer [53].

Blue emission for Zn(II) and Cu(II) complexes has been observed. The complexes, having the same molar concentrations as the ligands, display enhanced emission intensities compared to H_3L^1 and H_2L^2 when excited with similar energy. Enhancement of fluorescence through complexation is of much interest as it opens up the opportunity for photochemical applications of these complexes. The fluorescence of the free ligand is probably quenched by a photoinduced electron transfer process due to the presence of a lone pair on

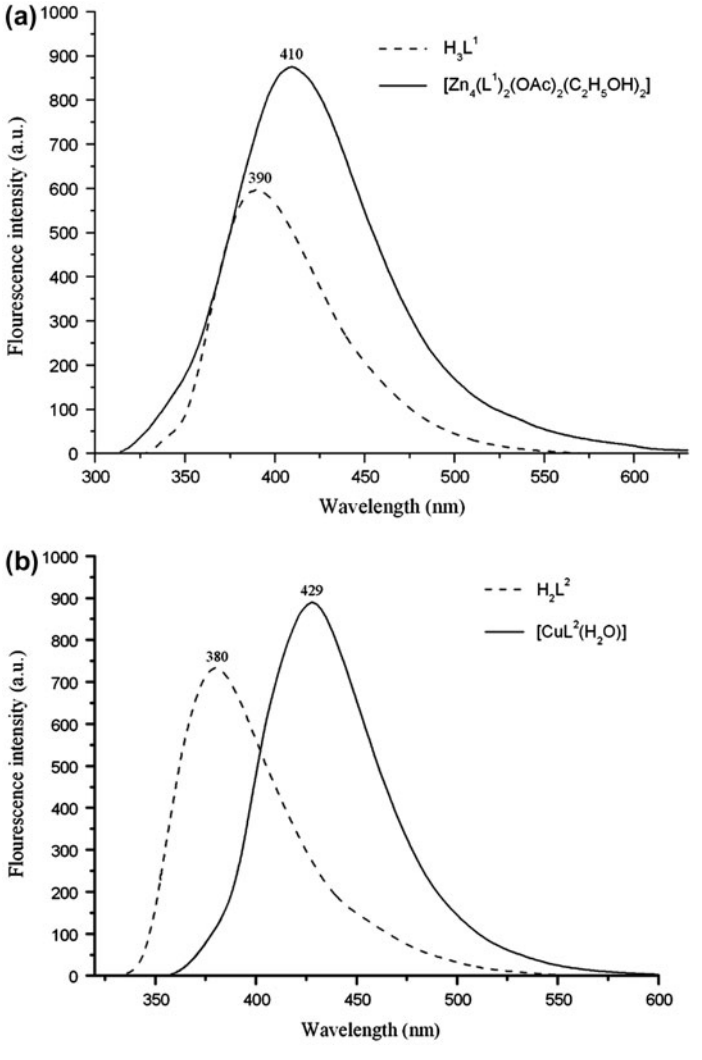

Figure 5. Emission spectra of the ligands and their corresponding complexes. (a) H_3L^1 (—) and its Zn(II) complex (—) in DMF ($C = 5 \times 10^{-5}$ mol L^{-1}, λ_{ex} = 330 and 335 nm, λ_{em} = 390 and 410 nm); (b) H_2L^2 (—) and its Cu(II) complex (—) in DMF ($C = 5 \times 10^{-5}$ mol L^{-1}, λ_{ex} = 330 and 335 nm, λ_{em} = 390 and 410 nm).

nitrogen. Such process is prevented by complexation of the ligands. Thus, the fluorescence intensity may be enhanced by coordination of Zn(II) and Cu(II). Chelation of the ligands to metal increases the rigidity of the ligands and thus reduces the loss of energy via vibrational motions, which may increase the emission efficiency.

The subtle changes of substituents of the ligand on spectroscopic properties of ligand and Zn(II) complexes are examined by the spectral behaviors of Zn(II) complex compared with that of the reported Zn(II) complex [21] (table 4). The characteristic C=N stretch is shifted to higher frequency by *ca.* 3 cm^{-1} for both free ligands and their Zn(II) complexes with the two Br-substituents (3,5-dibromo-2-hydroxybenzaldehyde) changing to one Cl-substituents (5-chloro-2-hydroxybenzaldehyde) in the ligands. In the UV–vis absorption spectra, the

Table 4. The spectral behaviors of the Zn(II) complex in this report and literature [21].

	IR spectra ($\nu_{C=N}$)/cm^{-1}		UV–vis absorption spectra/nm		Fluorescence spectra/nm	
Complex	Ligand	Zn(II) complex	Ligand	Zn(II) complex	Ligand	Zn(II) complex
This report	1615	1606	270, 323	284, 299, 365	390	410
Literature [21]	1612	1603	272, 320, 393	283, 368	411	423

absorption peaks have a significant change for both free ligands and their Zn(II) complexes. The emission peaks position is hypochromatic shifted for ligands and their complexes with the Br-substituents changing to Cl-substituents on the ligand. As a result, ligand substituents may control the spectral behavior of ligand and complexes.

4. Conclusions

$[Zn_4(L^1)_2(OAc)_2(CH_3CH_2OH)_2]$ and $[CuL^2(H_2O)]$ with asymmetric Salen-type bisoxime ligands have been synthesized and structurally characterized. In FT-IR spectra of the Zn(II) and Cu(II) complexes, ν_{M-O} and ν_{M-N} absorption frequencies have been observed. Meanwhile, the Zn(II) and Cu(II) complexes exhibit blue emission with the maximum emission wavelengths λ_{max} = 410 and 429 nm. The structures of the Zn(II) and Cu(II) complexes have distortion as a result of introduction of different substituents on benzene rings of the Salen-type bisoxime ligands. Comparison with previous work shows that changing the ligand substituents, while not completely changing structures, can regulate the spectral behaviors and supramolecular structures of ligand and its complexes.

Supplementary material

Further details of the crystal structure investigation(s) may be obtained from the Cambridge Crystallographic Data Centre, Postal Address: CCDC, 12 Union Road, CAMBRIDGE CB2 1EZ, UK. Telephone: (44) 01223 762910; Facsimile: (44) 01223 336033; E-mail: deposit@ccdc.cam.ac.uk on quoting the depository number CCDC Nos. 864126 and 864127 for the Zn(II) and Cu(II) complexes, respectively.

Acknowledgements

This work was supported by the National Natural Science Foundation of China, the Fundamental Research Funds for the Gansu Province Universities (212086) and the science and technology support funds of Lanzhou Jiaotong University (ZC2012003), which are gratefully acknowledged.

References

[1] N.S. Venkataramanan, G. Kuppuraj, S. Rajagopal. *Coord. Chem. Rev.*, **249**, 1249 (2005).
[2] T. Katsuki. *Coord. Chem. Rev.*, **140**, 189 (1995).
[3] L. Canali, D.C. Sherrington. *Chem. Soc. Rev.*, **28**, 85 (1999).

[4] T. Katsuki. *J. Mol. Catal. A: Chem.*, **113**, 87 (1996).
[5] S.S. Sun, C.L. Stern, S.T. Nguyen, J.T. Hupp. *J. Am. Chem. Soc.*, **126**, 6314 (2004).
[6] S.D. Bella, I. Fragala. *Synth. Met.*, **115**, 191 (2000).
[7] P.G. Lacroix. *Eur. J. Inorg. Chem.*, **2001**, 339 (2001).
[8] H. Dürr, H. Bouas-Laurent (Eds.). *Photochromism: Molecules and Systems; Studies in Organic Chemistry*, Vol. 40, Elsevier, Amsterdam (1990).
[9] M. Irie (Ed.). Photochromism: Memories and Switches, A Special Thematic Issue of Chemical Reviews, Vol. 100. p. 1685 (2000).
[10] Z.L. You, H.L. Zhu, W.S. Liu. *Z. Anorg. Allg. Chem.*, **630**, 1617 (2004).
[11] Z.L. You, H.L. Zhu. *Z. Anorg. Allg. Chem.*, **630**, 2754 (2004).
[12] K. Ogawa, T. Fujiwara. *Chem. Lett.*, **28**, 657 (1999).
[13] E. Ito, H. Oji, T. Araki, K. Oichi, H. Ishii, Y. Ouchi, T. Ohta, N. Kosugi, Y. Maruyama, T. Naito, T. Inabe, K. Seki. *J. Am. Chem. Soc.*, **119**, 6336 (1997).
[14] E. Hadjoudis, T. Dziembowska, Z. Rozadowski. *J. Photochem. Photobiol. A: Chem.*, **128**, 97 (1999).
[15] P. Cai, J.R. Hou, T.S. Liu, G.Z. Cheng, T.Y. Peng, Z.H. Peng. *Spectrochim*, *Acta, Part A*, **71**, 584 (2008).
[16] S. Akine, W.K. Dong, T. Nabeshima. *Inorg. Chem.*, **45**, 4677 (2006).
[17] W.K. Dong, J.G. Duan, Y.H. Guan, J.Y. Shi, C.Y. Zhao. *Inorg. Chim. Acta*, **362**, 1129 (2009).
[18] P.A. Vigato, S. Tamburini. *Coord. Chem. Rev.*, **248**, 1717 (2004).
[19] S. Akine, T. Taniguchi, W.K. Dong, S. Masubuchi, T. Nabeshima. *J. Org. Chem.*, **70**, 1704 (2005).
[20] Y.M. Jeon, J. Heo, C.A. Mirkin. *Tetrahedron Lett.*, **48**, 2591 (2007).
[21] W.K. Dong, S.J. Xing, Y.X. Sun, L. Zhao, L.Q. Chai, X.H. Gao. *J. Coord. Chem.*, **65**, 1212 (2012).
[22] G.J. Kim, J.H. Shin. *Catal. Lett.*, **63**, 83 (1999).
[23] E. Lamour, S. Routier, J.-L. Bernier, J.-P. Catteau, C. Bailly, H. Vezin. *J. Am. Chem. Soc.*, **121**, 1862 (1999).
[24] N.F. Choudhary, N.G. Connelly, P.B. Hitchcock, G.J. Leigh. *J. Chem. Soc., Dalton Trans.,* 4437 (1999).
[25] G. Verquin, G. Fontaine, M. Bria, E. Zhilinskaya, E. Abi-Aad, A. Aboukaïs, B. Baldeyrou, C. Bailly, J.-L. Bernier. *J. Biol. Inorg. Chem.*, **9**, 345 (2004).
[26] M.R. Bermejo, M.I. Fernández, A.M. González-Noya, M. Maneiro, R. Pedrido, M.J. Rodríguez, M. Vázquez. *Eur. J. Inorg. Chem.*, **2769**, (2004).
[27] U. Casellato, P. Guerriero, S. Tamburini, S. Sitran, P.A. Vigato. *J. Chem. Soc., Dalton Trans.,* 2145 (1991).
[28] A. Aguiari, E. Bullita, U. Casellato, P. Guerriero, S. Tamburini, P.A. Vigato. *Inorg. Chim. Acta*, **202**, 157 (1992).
[29] U. Casellato, P. Guerriero, S. Tamburini, P.A. Vigato, C. Benelli. *Inorg. Chim. Acta*, **207**, 39 (1993).
[30] M. Sakamoto, Y. Nishida, K. Ohhara, Y. Sadaoka, A. Matsumoto, H. Okawa. *Polyhedron*, **14**, 2505 (1995).
[31] M. Sakamoto, T. Ishikawa, Y. Nishida, Y. Sadaoka, A. Matsumoto, Y. Fukuda, M. Sakai, M. Ohba, H. Sakiyama, H. Okawa. *J. Alloys Compd.*, **238**, 23 (1996).
[32] H. Aono, M. Tsuzaki, A. Kawaura, M. Sakamoto, E. Traversa, Y. Sadaoka. *Chem. Lett.*, **28**, 1175 (1999).
[33] T. Le Borgne, E. Rivière, J. Marrot, P. Thuéry, J.-J. Girerd, M. Ephritikhine. *Chem.-Eur. J.,* **8**, 773 (2002).
[34] R. Miyamoto, T. Sugai, S. Sudoh. *Polyhedron*, **21**, 2127 (2002).
[35] H. Aono, N. Kondo, M. Sakamoto, E. Traversa, Y. Sadaoka. *J. Eur. Ceram. Soc.*, **23**, 1375 (2003).
[36] C.T. Zeyrek, A. Elmali, Y. Elerman. *J. Mol. Struct.*, **740**, 47 (2005).
[37] P. Guerriero, S. Tamburini, P.A. Vigato, U. Russo, C. Benelli. *Inorg. Chim. Acta*, **213**, 279 (1993).
[38] J. Sanmartín, M.R. Bermejo, A.M. García-Deibe, O. Piro, E.E. Castellano. *Chem. Commun.*, **1953**, (1999).
[39] The trigonality index τ (τ = 0 denotes ideal square pyramidal; τ = 1 denotes ideal trigonal bipyramidal) was calculated according to the literature. See: A.W. Addison, T.N. Rao, J. Reedijk, J. van Rijn, G.C. Verschoor. *J. Chem. Soc. Dalton Trans.,* 1349 (1984).
[40] W.K. Dong, C.Y. Zhao, Y.X. Sun, X.L. Tang, X.N. He. *Inorg. Chem. Commun.*, **12**, 234 (2009).
[41] W.K. Dong, Y.X. Sun, Y.P. Zhang, L. Li, X.N. He, X.L. Tang. *Inorg. Chim. Acta*, **362**, 117 (2009).
[42] A. Panja, N. Shaikh, P. Vojtišek, S. Gao, P. Banerjee. *New J. Chem.*, **26**, 1025 (2002).
[43] A. Anthonysamy, S. Balasubramanian. *Inorg. Chem. Commun.*, **8**, 908 (2005).
[44] T.Z. Yu, K. Zhang, Y.L. Zhao, C.H. Yang, H. Zhang, L. Qian, D.W. Fan, W.K. Dong, L.L. Chen, Y.Q. Qiu. *Inorg. Chim. Acta*, **361**, 233 (2008).
[45] J.A. Faniran, K.S. Patel, J.C. Bailar. *J. Inorg. Nucl. Chem.*, **36**, 1547 (1974).
[46] W.K. Dong, Y.X. Sun, C.Y. Zhao, X.Y. Dong, L. Xu. *Polyhedron*, **29**, 2087 (2010).
[47] W.K. Dong, X.N. He, H.B. Yan, Z.W. Lv, X. Chen, C.Y. Zhao, X.L. Tang. *Polyhedron*, **28**, 1419 (2009).
[48] G.C. Percy, J. Thornton. *J. Inorg. Nucl. Chem.*, **35**, 2319 (1973).
[49] S. Akine, Y. Morita, F. Utsuno, T. Nabeshima. *Inorg. Chem.*, **48**, 10670 (2009).
[50] H.E. Smith. *Chem. Rev.*, **83**, 359 (1983).
[51] L. Gomes, E. Pereira, B. de Castro. *J. Chem. Soc., Dalton Trans.,* 1373 (2000).
[52] C.Y. Guo, Y.Y. Wang, K.Z. Xu, H.L. Zhu, Q.Z. Shi, S.M. Peng. *Polyhedron*, **27**, 3529 (2008).
[53] G.B. Che, C.B. Liu, B. Liu, Q.W. Wang, Z.L. Xu. Crys. *Eng. Commun.*, **10**, 84 (2008).